THE ASTROPHYSICAL JOURNAL, 413:349–363, 1993 August 10

A SEARCH FOR SUBSTELLAR COMPANIONS TO SOUTHERN SOLAR-TYPE STARS

KAYLENE A. MURDOCH, J. B. HEARNSHAW, AND M. CLARK
Mount John University Observatory, Department of Physics and Astronomy, University of Canterbury, Private Bag 4800, Christchurch, New Zealand
Received 1993 January 21; accepted 1993 February 19

ABSTRACT

At the Mount John University Observatory relative radial velocities of solar-type stars have been obtained with a characteristic random error of 55 m s^{-1} using a fiber-fed echelle system and digital cross-correlation techniques. A program of obtaining radial velocities of 29 solar-type stars and 10 giant International Astronomical Union radial-velocity standard stars was carried out over 2.5 years with a view to the detection of low-mass companions to the dwarf stars. One dwarf star turned out to have a previously undiscovered stellar companion but no dwarfs showed radial-velocity variability suggestive of the presence of substellar companions, although one showed a possible variation. In contrast, at least half the giant or supergiant "standard" stars were variable in radial velocity. Four and possibly five of the giant standards are probably intrinsic (pulsating) red or yellow (Walker et al. 1989) variables. Two further standards showed long-period variability suggestive of companions of undetermined mass.

The lack of brown dwarfs observed in this program is consistent with the results of other recent surveys. High-mass brown dwarfs appear to be rare as companions to stars and are unlikely to contribute significantly to the local mass density. Low-mass brown dwarfs (or high-mass planets) seem to be rare in orbits closer than 10 AU but could yet be found to abound in wider orbits or in the field.

Subject headings: binaries: spectroscopic — stars: low-mass, brown dwarfs — stars: luminosity function, mass function

1. INTRODUCTION

In the last decade significant technical advances have been made which have permitted searches for substellar objects such as brown dwarfs (Tarter 1975). The methods used include photometric surveying of white dwarfs for infrared excess indicative of a cool companion (Kumar 1987; Zuckerman & Becklin 1987), infrared imaging either in the field (e.g., Jameson & Skillen 1989; Stauffer et al. 1989) or around stars (Jameson, Sherrington, & Giles 1983; Skrutskie, Forrest, & Shure 1986, 1989; Forrest, Skrutskie, & Shure 1988) and speckle interferometry (Henry & McCarthy 1990). Dynamical techniques have included searches for astrometric (Henry & McCarthy 1992) and radial-velocity (Campbell, Walker, & Yang 1988; Marcy & Benitz 1989) perturbations of stars which might indicate that they have substellar companions.

While the classification of faint, red images as either stellar or substellar has been complicated by uncertain theoretical predictions, distances, and reddenings, dynamical techniques involving astrometry or radial-velocity measurements are able to give an estimate of the mass of a companion to a star as a direct result of the orbital analysis.[1] The drawback is that one needs to make observations over a time scale comparable to the orbital period and with very high precision. For example, a brown dwarf (here defined as having a mass between about 20 M_{2l} and 80 M_{2l}) in orbit about a star of solar mass with period less than 10 years would induce a maximum radial-velocity perturbation in the primary of only a few tenths to about 5 km s^{-1}.

At the Mount John University Observatory a system was developed which has enabled radial velocities of bright solar-type stars to be obtained with a precision sufficient to detect brown-dwarf mass companions. This paper describes the results of a program of looking for such companions to a sample of southern solar-type stars.

[1] In the case of the radial-velocity technique, the result is usually a lower limit to the mass of the companion.

2. METHOD AND RESULTS

The Mount John program was described earlier by Murdoch & Hearnshaw (1991a). Briefly, the instrumentation comprised an echelle spectrograph and Reticon diode array connected by a single optical fiber feed to the Mount John University Observatory's 1 m McLellan telescope. The fiber feed enabled the spectrograph to be mounted in a thermally and mechanically stable environment. This, along with the reduction in guiding errors because of light scrambling in the fiber, was expected to improve radial-velocity precision to better than 100 m s^{-1}. Spectra of 29 solar-type dwarfs (spectral type between F5 and K5, $\delta < +10°$, $V < 5.0$) and 10 IAU standard stars (mostly giants) were obtained approximately monthly between 1988 November and 1991 September, with the exception of a 6 month interval when equipment failure prohibited observing. Relative radial velocities were obtained by digitally cross correlating the spectra of each star with a single ("template") spectrum of the same star. Corrections for each observing run, based on the mean relative velocity of stars of assumed constant velocity, were then applied.

The radial velocities of the Mount John program stars are listed in Table 1. So as to render the Mount John relative radial velocities more generally useful, corrections have been made so that the velocities are relative to the Sun rather than relative to the velocity of each star at the epoch when the template spectrum was recorded. To do this, the spectral template of each star in the Mount John program has been cross-correlated with the template of one of three IAU radial-velocity standard stars. The actual IAU standard star template chosen is the one closest in spectral type to the star itself, in

TABLE 1

RADIAL VELOCITIES OF THE MOUNT JOHN PROGRAM STARS

HJD −2440000	Velocity (km s^{-1})	HJD −2440000	Velocity (km s^{-1})	HJD −2440000	Velocity (km s^{-1})	HJD −2440000	Velocity (km s^{-1})	HJD −2440000	Velocity (km s^{-1})
HR 77 (ζ Tuc)		8087.10	+12.365	7520.08	− 6.916	7965.89	−13.622	7592.01	+26.068
7479.97	+ 9.721	8132.19	+12.369	7549.91	− 6.812	7999.80	−13.683	7639.88	+27.002
7480.93	+ 9.825	8146.12	+12.286	7570.90	− 7.039	8021.79	−13.681	7643.97	+26.869
7519.95	+ 9.701	8176.06	+12.390	7610.88	− 6.821	8091.24	−13.676	7693.89	+27.811
7550.93	+ 9.761	8220.97	+12.221	7729.26	− 6.897	8133.18	−13.619	7728.84	+28.052
7606.88	+ 9.849	8232.99	+12.396	8083.20	− 6.855	8146.25	−13.652	7944.02	+27.666
7652.07	+ 9.747	8258.92	+12.236	8133.09	− 6.915	8147.16	−13.703	8018.84	+22.392
7729.19	+ 9.767	8322.89	+12.172	8147.08	− 6.898	8176.14	−13.635	8019.84	+26.203
7946.90	+ 9.905	8423.24	+12.442	8148.12	− 6.989	8180.98	−13.621	8020.81	+26.042
8000.21	+ 9.643	HR 911 (α Cet)		8175.13	− 6.913	8182.12	−13.672	8061.89	+25.011
8087.06	+ 9.765	7480.08	−25.097	8176.10	− 6.934	8220.08	−13.678	8132.84	+23.196
8132.12	+ 9.726	7482.09	−25.203	8221.05	− 7.026	8221.07	−13.773	8147.20	+23.119
8148.08	+ 9.679	7519.99	−25.366	8256.92	− 6.880	8256.98	−13.688	8181.02	+22.624
8176.05	+ 9.902	7529.92	−25.459	8258.89	− 6.940	8259.99	−13.668	8220.13	+22.120
8219.99	+ 9.688	7547.91	−25.113	8259.95	− 6.918	8306.95	−13.654	8257.06	+22.357
8232.95	+ 9.742	7552.93	−25.515	8308.87	− 6.902	8322.94	−13.686	8259.12	+22.203
8259.02	+ 9.715	7570.88	−25.588	8323.86	− 6.877	8323.96	−13.596	8260.06	+22.173
8308.86	+ 9.663	7571.88	−25.549	8325.89	− 6.889	8325.90	−13.672	8307.94	+22.569
8321.90	+ 9.892	7729.24	−25.363	8441.26	− 6.874	8373.80	−13.635	8320.92	+23.151
8374.90	+ 9.928	8131.20	−24.976	8479.15	− 6.855	8386.80	−13.636	8322.02	+23.226
8421.26	+ 9.914	8146.18	−25.134	HR 1674 (ζ Dor)		8479.24	−13.623	8324.99	+23.011
8441.19	+ 9.774	8147.17	−25.099	7480.12	− 0.690	HR 1983 (γ Lep)		8374.78	+23.914
8477.83	+ 9.783	8175.10	−24.952	7520.93	− 0.728	7482.02	− 8.814	8419.82	+24.811
8478.82	+ 9.665	8176.09	−25.003	7570.94	− 0.765	7521.04	− 8.766	8420.79	+24.846
HR 98 (β Hyi)		8219.90	−25.304	7603.95	− 0.645	7546.99	− 8.771	8440.77	+24.946
7480.90	+23.581	8232.91	−25.000	7640.85	− 0.898	7571.00	− 8.603	HR 3748 (α Hya)	
7519.98	+23.557	8256.91	−24.926	7653.83	− 0.744	7591.90	− 8.700	7490.11	− 3.117
7549.01	+23.670	8306.89	−25.319	7943.96	− 0.621	7946.98	− 8.844	7520.10	− 3.224
7571.91	+23.727	8321.86	−25.483	8091.20	− 0.651	7965.87	− 8.687	7521.15	− 3.250
7602.94	+23.487	8323.84	−25.308	8131.24	− 0.829	8133.20	− 8.710	7529.12	− 3.216
7652.03	+23.620	8325.86	−25.279	8147.06	− 0.745	8221.12	− 8.831	7547.07	− 3.321
7694.28	+23.580	8441.27	−25.294	8181.05	− 0.744	8256.96	− 8.732	7548.08	− 3.302
7729.21	+23.614	8443.29	−25.191	8221.09	− 1.024	8259.97	− 8.644	7549.03	− 3.269
8000.17	+23.461	8479.22	−25.182	8257.00	− 0.722	8306.93	− 9.081	7551.07	− 3.353
8086.25	+23.596	HR 1008 (82 Eri)		8321.99	− 0.720	8323.90	− 8.690	7553.08	− 3.180
8132.14	+23.562	7480.05	+81.255	8373.82	− 0.901	HR 2906		7554.99	− 3.263
8146.08	+23.592	7518.03	+81.137	8386.86	− 0.977	7487.11	+61.590	7571.03	− 3.268
8176.08	+23.511	7551.00	+81.213	8420.77	− 0.782	7521.07	+61.621	7591.96	− 3.386
8219.94	+23.371	7571.95	+81.344	HR 1743 (o Col)		7551.10	+61.448	7602.83	− 3.327
8232.97	+23.631	7610.85	+81.245	7481.11	+20.356	7591.93	+61.285	7603.82	− 3.409
8259.05	+23.456	7943.91	+81.257	7520.98	+20.248	7643.91	+61.666	7604.83	− 3.421
8306.86	+23.597	7964.87	+81.235	7547.97	+20.202	7944.97	+61.610	7605.83	− 3.381
8320.89	+23.648	8091.15	+81.153	7603.88	+20.399	7965.92	+61.587	7610.91	− 3.331
8321.88	+23.719	8132.98	+81.154	7643.85	+20.353	7999.86	+61.603	7639.95	− 3.430
8322.87	+23.652	8146.16	+81.103	7964.95	+20.307	8021.84	+61.600	7640.82	− 3.200
8323.87	+23.595	8181.08	+81.095	8133.13	+20.300	8133.23	+61.642	7643.89	− 3.325
8324.87	+23.575	8221.00	+81.064	8147.11	+20.280	8147.23	+61.611	7690.78	− 3.418
8325.88	+23.600	8233.02	+81.200	8181.13	+20.258	8182.10	+61.642	7693.81	− 3.350
8373.01	+23.669	8258.97	+81.200	8256.94	+20.321	8257.03	+61.510	7699.86	− 3.273
8384.82	+23.608	8306.91	+81.126	8260.01	+20.318	8260.03	+61.435	7724.82	− 3.329
8386.82	+23.573	8322.92	+81.074	8308.90	+20.379	8306.98	+61.550	7965.07	− 3.326
8421.24	+23.598	8443.30	+81.108	8323.89	+20.364	8323.92	+61.513	7999.89	− 3.294
8441.21	+23.533	HR 1083 (κ Ret)		8479.19	+20.302	8373.84	+61.632	8018.80	− 3.233
HR 188 (β Cet)		7481.05	+14.368	HR 1829 (β Lep)		HR 2943 (α CMi)		8019.80	− 3.378
7479.99	+13.628	7520.04	+14.236	7480.15	−13.492	7481.17	− 3.199	8020.85	− 3.332
7480.95	+13.597	7551.05	+14.322	7481.15	−13.628	7518.13	− 3.260	8061.86	− 3.379
7481.99	+13.621	7609.89	+14.509	7487.07	−13.624	7547.05	− 3.210	8181.22	− 3.322
7489.95	+13.665	7643.81	+14.402	7518.06	−13.711	7571.02	− 3.233	8308.01	− 3.076
7519.92	+13.420	7729.93	+14.277	7520.89	−13.596	7591.97	− 3.321	8322.07	− 3.198
7528.97	+13.527	7944.91	+14.516	7521.02	−13.672	7945.00	− 3.091	8372.77	− 3.042
7729.17	+13.553	8000.12	+14.499	7547.03	−13.727	7965.94	− 3.097	8373.88	− 3.134
7730.15	+13.529	8091.10	+14.444	7548.90	−13.608	7998.83	− 3.141	8374.91	− 3.067
8086.23	+13.544	8133.05	+14.276	7549.93	−13.497	8021.81	− 3.100	8385.00	− 3.065
8132.15	+13.552	8146.22	+14.319	7550.96	−13.670	8133.26	− 3.093	8419.76	− 3.165
8133.01	+13.563	8176.12	+14.211	7551.97	−13.647	8181.18	− 3.070	8420.76	− 3.136
8146.09	+13.536	8221.03	+14.187	7570.98	−13.671	8257.04	− 3.018	8425.75	− 3.268
8176.09	+13.511	8233.06	+14.308	7571.99	−13.736	8260.04	− 3.033	8441.76	− 3.177
8219.96	+13.401	8259.00	+14.827	7591.88	−13.631	8306.96	− 2.939	8442.76	− 3.278
8232.94	+13.533	8308.95	+14.336	7606.84	−13.643	8323.93	− 2.955	HR 3862	
8423.31	+13.595	8321.96	+14.235	7609.84	−13.640	8372.79	− 2.861	7489.07	+35.190
8441.28	+13.572	8374.87	+14.017	7943.87	−13.626	HR 3220		7529.07	+35.068
HR 370 (ν Phe)		8423.28	+ 14.618	7944.87	−13.642	7489.00	+24.355	7555.03	+35.234
7481.96	+12.148	HR 1136 (δ Eri)		7947.01	−13.645	7529.01	+24.781	7654.98	+35.200
7517.97	+12.333	7480.01	− 6.938	7964.90	−13.673	7548.04	+25.248	7699.80	+35.207

TABLE 1—*Continued*

HJD −2440000	Velocity (km s^{-1})	HJD −2440000	Velocity (km s^{-1})	HJD −2440000	Velocity (km s^{-1})	HJD −2440000	Velocity (km s^{-1})	HJD −2440000	Velocity (km s^{-1})
HR 3862 (cont.)		8373.05	+ 4.959	8420.84	+21.734	8442.85	− 7.049	7996.83	−19.567
7965.02	+35.186	8374.96	+ 4.970	8420.95	+21.659	HR 5459 (α Cen A)		7997.98	−19.590
7999.92	+35.200	8384.88	+ 5.044	8421.06	+21.598	7487.15	−23.743	7998.00	−19.555
8020.89	+35.046	8386.96	+ 4.987	8422.77	+21.899	7520.12	−23.901	7998.02	−19.562
8061.82	+35.123	8420.86	+ 5.045	8423.00	+21.842	7548.11	−23.933	8000.06	−19.544
8086.82	+35.128	8422.84	+ 5.026	8423.16	+21.863	7603.11	−23.944	8020.00	−19.615
8181.20	+35.100	8441.80	+ 4.923	8425.77	+22.363	7649.15	−23.930	8061.99	−19.635
8257.12	+35.204	8442.77	+ 5.058	8426.10	+22.368	7690.95	−23.811	8083.04	−19.627
8308.97	+35.406	HR 4763 (γ Cru)		8440.81	+22.438	7725.01	−23.883	8130.84	−19.575
8322.04	+35.134	7487.17	+22.697	8440.98	+22.555	7945.21	−23.759	8130.90	−19.635
8374.84	+35.145	7530.08	+22.863	8441.87	+22.617	7996.04	−23.770	8146.93	−19.591
8384.92	+35.283	7555.13	+23.056	8441.94	+22.659	7996.82	−23.756	8147.96	−19.651
8420.82	+35.147	7602.96	+22.529	8442.80	+22.739	7997.97	−23.764	8181.86	−19.674
8441.78	+35.156	7603.99	+22.616	8442.92	+22.736	7997.99	−23.757	8259.08	−19.741
HR 4134		7606.02	+22.846	8478.98	+22.136	7998.01	−23.772	8260.10	−19.675
7490.00	+21.278	7640.09	+22.629	HR 4786 (β Crv)		8000.05	−23.739	8307.09	−19.853
7530.03	+21.643	7648.79	+22.651	7592.05	− 7.186	8019.99	−23.788	8308.05	−19.942
7555.09	+21.838	7651.91	+22.451	7604.12	− 7.221	8061.98	−23.802	8322.02	−19.742
7604.03	+21.847	7644.00	+22.533	7652.00	− 7.180	8083.01	−23.764	8322.15	−19.731
7644.04	+21.530	7653.98	+22.357	7693.93	− 7.140	8130.83	−23.753	8323.04	−19.814
7702.86	+21.560	7650.96	+22.569	7723.83	− 7.248	8130.89	−23.765	8323.14	−19.652
7724.86	+21.844	7690.93	+22.627	7944.07	− 7.137	8131.82	−23.735	8323.99	−19.633
7945.15	+21.617	7699.97	+22.475	7945.01	− 7.192	8131.82	−23.758	8324.07	−19.655
7999.99	+21.780	7729.86	+22.147	7965.17	− 7.183	8131.83	−23.782	8324.96	−19.650
8019.92	+21.992	7946.94	+22.050	7966.00	− 7.179	8131.83	−23.757	8325.06	−19.633
8061.94	+21.445	7965.21	+22.384	7995.92	− 7.144	8131.84	−23.763	8325.96	−19.650
8086.92	+21.970	7998.04	+22.076	7996.06	− 7.195	8131.85	−23.770	8368.82	−19.750
8086.92	+21.970	8000.15	+22.218	7997.94	− 7.153	8131.85	−23.776	8372.82	−19.610
8147.25	+21.572	8061.97	+22.233	8000.03	− 7.206	8131.87	−23.794	8374.94	−19.675
8182.14	+21.933	8082.86	+22.869	8000.07	− 7.123	8131.88	−23.780	8384.84	−19.708
8257.10	+22.001	8083.05	+22.880	8085.82	− 7.208	8131.89	−23.785	8384.94	−19.697
8308.07	+21.793	8086.96	+22.283	8090.83	− 7.236	8131.90	−23.792	8385.14	−19.709
8322.09	+21.823	8130.92	+22.685	8146.80	− 7.176	8131.90	−23.759	8386.93	−19.672
8372.91	+21.635	8132.93	+22.552	8309.10	− 7.226	8131.91	−23.704	8419.79	−19.706
8385.01	+21.756	8146.94	+22.832	8325.03	− 7.165	8146.92	−23.720	8420.02	−19.624
8419.84	+21.792	8147.93	+22.774	HR 4979		8181.86	−23.770	8420.99	−19.722
8440.79	+21.702	8181.17	+22.380	7553.05	−12.412	8259.07	−23.731	8421.07	−19.696
HR 4523		8181.87	+22.284	7606.13	−12.567	8260.09	−23.735	8423.05	−19.696
7490.08	+17.525	8221.12	+22.747	7640.04	−12.412	8307.08	−23.644	8423.18	−19.720
7552.97	+17.291	8257.08	+22.373	7651.97	−12.443	8308.04	−23.600	8425.92	−19.732
7606.06	+17.467	8259.06	+22.920	7702.94	−12.532	8322.01	−23.756	8426.11	−19.379
7653.91	+17.708	8259.11	+22.915	7724.93	−12.434	8322.14	−23.769	8440.88	−19.712
7690.87	+17.567	8260.08	+23.073	7965.12	−12.488	8323.04	−23.802	8441.89	−19.726
7728.91	+17.458	8307.04	+22.778	7995.99	−12.516	8323.13	−23.650	8442.82	−19.779
7944.13	+17.490	8307.06	+22.632	8020.05	−12.530	8323.98	−23.660	8478.99	−19.709
7995.96	+17.519	8309.09	+23.045	8082.97	−12.547	8324.06	−23.681	HR 5777 (37 Lib)	
8020.95	+17.436	8321.91	+22.589	8132.90	−12.520	8324.95	−23.666	7606.22	+49.114
8082.90	+17.486	8322.13	+22.673	8146.89	−12.421	8325.05	−23.675	7651.06	+49.114
8133.83	+17.387	8323.07	+22.758	8260.14	−12.471	8325.95	−23.684	7693.98	+49.146
8146.84	+17.329	8323.14	+22.735	8309.05	−12.353	8368.81	−23.690	7728.99	+49.131
8182.18	+17.631	8323.97	+22.792	8323.20	−12.501	8372.81	−23.628	7996.11	+49.122
8257.17	+17.506	8324.08	+22.779	8372.98	−12.427	8374.93	−23.672	8020.12	+49.072
8309.00	+17.615	8324.89	+22.725	8375.01	−12.466	8384.84	−23.669	8085.90	+49.147
8323.17	+17.503	8325.02	+22.738	8385.04	−12.380	8384.94	−23.685	8133.94	+49.090
8372.96	+17.520	8325.07	+22.710	8420.92	−12.608	8385.13	−23.658	8147.86	+49.160
8374.98	+17.503	8325.14	+22.743	8425.89	−12.484	8386.92	−23.651	8309.15	+49.057
8384.97	+17.529	8325.94	+22.566	8440.84	−12.465	8387.05	−23.698	8372.08	+49.148
8422.87	+17.526	8368.80	+21.886	HR 5019 (61 Vir)		8419.78	−23.602	8373.13	+49.142
HR 4540 (β Vir)		8368.84	+21.853	7553.13	− 6.865	8420.01	−23.626	8375.07	+49.033
7530.11	+ 4.912	8368.86	+21.826	7603.06	− 6.810	8420.98	−23.672	8419.95	+48.975
7555.15	+ 5.036	8371.93	+22.050	7609.95	− 6.918	8421.07	−23.694	8422.97	+49.127
7603.00	+ 5.032	8372.19	+22.068	7651.00	− 6.949	8423.04	−23.622	8425.96	+49.018
7651.94	+ 5.108	8372.80	+22.228	7729.83	− 6.977	8425.92	−23.641	8440.91	+49.341
7690.81	+ 4.975	8373.04	+22.102	7966.08	− 7.234	8426.11	−23.660	8441.91	+49.128
7729.80	+ 4.994	8373.89	+22.202	7996.08	− 6.898	8441.89	−23.700	8442.87	+49.125
7945.10	+ 4.944	8374.79	+22.340	8021.03	− 7.070	8442.81	−23.640	HR 6056 (δ Oph)	
7966.03	+ 4.995	8374.92	+22.324	8085.86	− 6.867	8478.99	−23.648	7604.24	−18.675
7997.92	+ 4.950	8375.03	+22.290	8133.88	− 6.842	HR 5460 (α Cen B)		7606.18	−18.798
8085.80	+ 5.021	8375.17	+22.344	8147.82	− 6.953	7487.15	−19.316	7651.11	−18.862
8090.80	+ 4.980	8384.83	+21.925	8260.16	− 6.909	7520.13	−19.395	7652.11	−18.696
8259.15	+ 5.111	8384.95	+21.930	8309.11	− 7.086	7548.12	−19.425	7690.99	−18.919
8309.02	+ 4.959	8385.16	+21.885	8323.09	− 6.929	7603.12	−19.437	7702.99	−18.739
8321.99	+ 4.897	8386.90	+21.845	8373.07	− 6.834	7649.16	−19.504	7724.98	−18.864
8323.05	+ 5.004	8387.08	+21.850	8385.07	− 6.987	7690.96	−19.479	7728.95	−19.212
8323.94	+ 5.065	8419.77	+21.803	8420.89	− 7.024	7725.02	−19.505	7743.91	−18.986
8325.09	+ 5.054	8419.91	+21.823	8422.93	− 6.968	7945.22	−19.515	8132.95	−18.880
8325.91	+ 4.963	8420.00	+21.806	8440.86	− 6.885	7996.05	−19.570	8145.82	−18.879

TABLE 1—*Continued*

HJD −2440000	Velocity (km s^{-1})	HJD −2440000	Velocity (km s^{-1})	HJD −2440000	Velocity (km s^{-1})	HJD −2440000	Velocity (km s^{-1})	HJD −2440000	Velocity (km s^{-1})
HR 6056 (cont.)		8426.02	+ 6.378	7700.12	−19.697	8375.12	−21.113	8176.89	+ 6.646
8147.90	−18.914	8440.93	+ 6.421	7729.11	−19.403	8421.09	−21.124	8176.90	+ 6.804
8309.17	−19.125	8441.96	+ 6.399	8021.19	−17.499	8423.09	−21.123	8180.99	+ 6.562
8322.12	−19.167	8442.89	+ 6.410	8062.10	−17.257	8441.10	−21.115	8182.00	+ 6.680
8323.11	−19.087	HR 6603 (β Oph)		8085.97	−17.137	8442.04	−21.175	8220.93	+ 6.550
8323.16	−19.116	7649.14	−11.959	8090.93	−17.105	8442.94	−21.173	8420.21	+ 6.816
8324.09	−19.151	7729.07	−11.973	8131.00	−16.867	8479.08	−21.153	8421.22	+ 6.892
8325.12	−18.995	7996.14	−11.912	8145.85	−16.819	HR 8181 (γ Pav)		8423.15	+ 6.763
8372.10	−19.044	8020.17	−11.967	8180.94	−16.711	7486.96	−29.290	8441.13	+ 6.849
8373.09	−19.022	8062.05	−12.000	8372.23	−15.759	7604.20	−29.318	8478.93	+ 6.803
8375.09	−18.876	8083.12	−11.935	8420.05	−15.507	7652.15	−29.619	HR 8387 (ϵ Ind)	
8385.10	−19.136	8085.94	−11.991	8441.08	−15.571	7694.16	−29.518	7487.02	−39.697
8387.10	−18.970	8090.90	−11.996	8442.01	−15.565	7725.16	−29.593	7528.94	−39.545
8419.92	−19.053	8322.20	−12.032	8479.03	−15.373	7744.00	−29.408	7700.23	−39.657
8420.87	−18.983	8147.91	−12.019	HR 7602 (β Aql)		8021.26	−29.395	7730.18	−39.601
8420.97	−18.980	8372.20	−11.985	7652.26	−39.881	8083.24	−29.391	8086.11	−39.569
8422.90	−18.996	8373.11	−12.064	7692.14	−39.889	8131.10	−29.505	8131.15	−39.579
8423.01	−19.062	8375.10	−11.991	7729.97	−39.928	8145.94	−29.495	8145.98	−39.545
8425.99	−19.074	8387.16	−11.953	8021.14	−39.872	8176.03	−29.229	8176.96	−39.666
8426.05	−19.008	8420.08	−12.080	8062.15	−39.920	8176.94	−29.418	8182.03	−39.528
8440.94	−19.098	8421.05	−12.026	8086.01	−39.895	8181.98	−29.420	8258.95	−39.595
8440.96	−19.113	8423.03	−12.024	8131.93	−39.954	8259.94	−29.664	8324.14	−39.513
8441.03	−18.994	8426.07	−12.077	8145.88	−39.943	8309.21	−29.419	8373.21	−39.623
8441.93	−19.072	8441.01	−11.950	8147.97	−39.910	8324.04	−29.550	8421.14	−39.633
8441.98	−19.045	8442.96	−12.059	8181.92	−39.973	8373.19	−29.525	8441.15	−39.465
8442.90	−19.145	8479.02	−12.007	8372.17	−39.896	8375.15	−29.472	8479.12	−39.574
8478.97	−18.913	HR 6859 (δ Sgr)		8375.19	−39.821	8420.18	−29.177	HR 8447 (τ PsA)	
HR 6102 (γ Aps)		7649.18	−19.869	8420.13	−39.966	8441.11	−29.416	7703.04	−15.546
7482.07	+ 6.312	7652.23	−19.873	8421.11	−39.851	8442.95	−29.525	7725.20	−15.928
7529.97	+ 6.528	7692.09	−19.742	8423.13	−39.906	8479.09	−29.269	8062.19	−16.072
7603.17	+ 6.375	7694.09	−19.801	8441.04	−39.861	HR 8232 (β Aqr)		8087.00	−16.074
7610.98	+ 6.538	7700.08	−19.783	8442.02	−39.951	7479.87	+ 7.014	8132.07	−16.112
7649.10	+ 6.359	8021.08	−19.715	8479.06	−39.956	7480.88	+ 6.828	8146.02	−15.834
7691.03	+ 6.464	8062.13	−19.757	HR 7665 (δ Pav)		7481.87	+ 6.907	8176.99	−15.441
7729.05	+ 6.454	8086.03	−19.736	7604.16	−21.157	7486.92	+ 6.846	8182.05	−16.036
7996.18	+ 6.456	8131.98	−19.782	7649.21	−21.152	7487.95	+ 7.027	8373.24	−16.123
8020.21	+ 6.482	8145.90	−19.832	7692.19	−21.172	7488.95	+ 6.991	8420.24	−16.012
8083.09	+ 6.454	8181.94	−19.760	7729.14	−21.111	7694.26	+ 6.733	8421.18	−15.115
8130.95	+ 6.446	8324.11	−19.727	7965.20	−21.090	7725.12	+ 6.524	8441.17	−15.785
8146.97	+ 6.443	8372.21	−19.764	8021.11	−21.150	7730.00	+ 6.767	HR 8969 (ι Psc)	
8181.90	+ 6.417	8420.10	−19.746	8086.06	−21.137	8021.23	+ 6.512	7479.90	+ 5.996
8257.16	+ 6.380	8423.11	−19.725	8131.07	−21.107	8062.21	+ 6.540	7730.08	+ 6.109
8309.14	+ 6.535	8426.13	−19.699	8145.92	−21.112	8086.16	+ 6.714	8086.19	+ 6.194
8322.17	+ 6.471	8441.06	−19.704	8176.91	−21.115	8087.03	+ 6.810	8091.05	+ 6.126
8373.03	+ 6.391	8441.99	−19.755	8181.96	−21.119	8090.97	+ 6.708	8132.02	+ 6.110
8375.05	+ 6.480	8443.01	−19.736	8259.92	−21.162	8131.04	+ 6.624	8147.01	+ 6.102
8387.14	+ 6.465	8478.95	−19.781	8309.19	−21.131	8132.00	+ 6.557	8148.01	+ 6.048
8419.98	+ 6.519	HR 7597 (ω Sgr)		8324.01	−21.046	8145.96	+ 6.662	8177.01	+ 6.129
8421.00	+ 6.485	7487.91	−22.733	8372.25	−21.177	8147.03	+ 6.757	8182.08	+ 6.048
8423.06	+ 6.519	7488.91	−22.764	8373.16	−21.116	8148.04	+ 6.639	8421.29	+ 6.422

order to minimize the systematic error resulting from cross-correlation of spectra of different spectral type. The IAU standard stars chosen to calculate the absolute velocities had radial velocities that appeared to be constant with time and represented the range of spectral types of stars in the program. The resulting radial-velocity difference between each pair of templates, combined with the respective run correction for each template, the difference of the mean of the standard star velocities from the standard-star template and the IAU-accepted absolute radial velocity for the standard, has been added to each velocity for the star in order to convert it to a frame of reference relative to the solar system barycenter.

In five cases, stars in the program had stellar companions which induced relatively large-amplitude changes in the radial velocities of the stars. These stars were α Cen A and α Cen B (in their common orbit) and α CMi (Procyon) which are well-known binaries with good visual orbits; ω Sgr which is a known spectroscopic binary with no published orbit, and HR 3220, which was discovered to be a spectroscopic binary with a stellar companion during the course of this program. In order to examine the velocities of these stars for the presence of yet lower level radial-velocity variability, the orbital motion with the stellar companion was subtracted from the data. In the case of the α Cen system, the best-fit slopes in the velocity data sets of α Cen A and α Cen B were subtracted, after confirming that these slopes were consistent with the published orbit of Heintz (1982). Similarly the best-fit slope of the Procyon velocities, which was consistent with the orbit of Irwin et al. (1992), was subtracted from the Procyon velocities. Since ω Sgr has no published orbit and its period is considerably longer than the span of the Mount John observations (1000 days), no orbit could be obtained in this program; a fifth-order best-fit polynomial was subtracted instead. In the case of HR 3220, which has an orbit with a period of 900 days, orbital elements could be calculated from Mount John program data. The orbit is presented elsewhere (Murdoch & Hearnshaw 1993) and it is this orbit which was subtracted from the data before analysis in the following sections.

3. PERFORMANCE

3.1. *Possible Sources of Error*

In the Mount John program, the overall random error in the measurement of a radial velocity, ϵ_v, results from the uncertainty from photon noise ϵ_p, the uncertainty in the determination of the zero point of the dispersion solution $\epsilon_{\rm disp}$, the uncertainty in the determination of the run correction $\epsilon_{\rm run}$, perturbations from instrumental effects $\epsilon_{\rm instr}$ (such as thermal drifts in the spectrograph during the exposure), and the uncertainty in the barycentric correction $\epsilon_{\rm bc}$. If these sources of uncertainty are independent and normally distributed and the various ϵ represent the standard deviations of the noise Gaussians then ϵ_v is given by

$$\epsilon_v^2 = \epsilon_{\rm p}^2 + \epsilon_{\rm disp}^2 + \epsilon_{\rm run}^2 + \epsilon_{\rm instr}^2 + \epsilon_{\rm bc}^2 . \quad (1)$$

3.1.1. *Error From Photon Noise,* $\epsilon_{\rm p}$

During most of the Mount John program, the aim was to record spectra with a signal-to-noise ratio of 30:1 in order to expose for the minimum time and yet have a photon-noise limited radial-velocity error that was still only a minor contribution to the overall radial-velocity error bar ($\epsilon_{\rm p} \approx 15$ m s^{-1}). Calculation of the implied contribution to the total radial-velocity error from photon noise (see Murdoch & Hearnshaw 1991b) for real exposures during the observing runs in 1991 March and 1991 April showed that $\epsilon_{\rm p}$ was at most 10 m s^{-1} even for the broader lined stars, probably because observers tended to err on the side of obtaining a higher signal-to-noise ratio than the target of 30:1—in many cases the signal-to-noise ratio was 100:1.

3.1.2. *Error in the Dispersion Solution,* $\epsilon_{\rm disp}$

The quadratic polynomial $n = a_0 + a_1 \lambda + a_2 \lambda^2$ used to characterize the dispersion of the Mount John spectra relates the pixel number n to the central wavelength λ of that pixel. Of the coefficients a_0, a_1, and a_2, the most important for high-precision radial velocities is a_0. This term quantifies the zero point of the stellar spectrum on the array and is therefore crucial in determining the position of the cross-correlation function peak and ultimately the relative radial velocity. Random error in a_0 will translate into a random error in the measured velocity. Errors in higher-order coefficients will merely broaden the cross-correlation function—a much smaller, second-order effect in decreasing the precision.

In the Mount John system, the dispersion polynomial is obtained by first least-squares fitting Gaussian functions to the 14 individual Th-Ar reference emission spectrum lines to obtain their positions and then chi-squares fitting those line positions against the known line wavelengths. The source of random error in this process is the photon noise in the Th-Ar spectrum, which translates into uncertainty in the line positions.

The precision with which the position of each Th-Ar emission line is determined depends on the strength of the line. The quadratic weighting favors the stronger lines which have better defined positions so that, although some line positions are determined to a precision of only ± 300 m s^{-1}, the precision with which a_0 is determined from two comparison spectra (comparison spectra are obtained both before and after the stellar spectrum) corresponds typically to about ± 8 m s^{-1}.

3.1.3. *Error in Run Zero Point,* $\epsilon_{\rm run}$

It was found necessary to apply a correction to the Mount John velocities (Murdoch & Hearnshaw 1991a), which had a value dependent on the monthly observing run in which the observations were made. The implication is that the instrumental setup for each run induces a systematic error to the radial velocities of that run.

The most likely variation in the run-to-run setup of the system that could plausibly affect the relative radial velocities is the way the fiber end is imaged relative to the spectrograph slit. The fiber end is interfaced to the spectrograph via a plate attached by three sets of antagonistic screws. The placement of the fiber-end image on the slit is adjusted by the tweaking of these screws so that the image is centered on the slit, as judged by the appearance of the fiber end image reflected off the slit jaws into the slit viewing microscope. In practice however, the position of the fiber-end image on the slit may not have been symmetrical because of the difficulty of fine adjustment of the screws and because the placement is performed by eye. The asymmetry of the placement across the width of the slit will be different from run to run. The effect on the spectra in a run will be a characteristic asymmetry in the instrumental profile and therefore in the line profiles as well. In the Mount John system, since each spectrum is cross correlated with a template spectrum obtained during an earlier run, cross correlations generally involve two spectra with different line asymmetries. The results are asymmetrical cross-correlation peaks. Since symmetrical Gaussian functions are fitted to the peaks to obtain radial velocities, a systematic radial-velocity error will thereby occur for velocities in a given run.

A more subtle effect that may also contribute to the difference between run zero points is that of uneven radial distribution of light at the fiber output end. Barden (1988) has noted the near-perfect azimuthal scrambling of light at the output end of a fiber, but the poorer radial scrambling. For example, an off-axis spot of light at the input end may appear as a ring of light at the output end. This may introduce zonal errors in the spectrograph which have a characteristic effect from run to run.

This systematic error for velocities in a given run is in part corrected for by determining the mean value of the radial velocities of presumed constant radial-velocity stars, as described by Murdoch & Hearnshaw (1991a). The value of the systematic error for each run is determined with a random error, which over all the runs translates into a pseudo-random error contribution $\epsilon_{\rm run}$ to ϵ_v. On average, 10 velocities are used to establish the zero point for each run. From the scatter in these velocities about the implied run correction (mean value of these velocities) it is found that the mean error in the run correction $\epsilon_{\rm run}$ is about 17 m s^{-1}.

3.1.4. *Errors from Instrumental Sources,* $\epsilon_{\rm instr}$

Although the optical fiber feed is used to reduce the errors from the instrumental sources which traditionally limit the precision of radial velocities (Griffin & Griffin 1973), these errors still exist and contribute to the uncertainty in the determination of radial velocities. They comprise mainly thermal and barometric changes which cause shifts in the zero point of the system. Figure 1 illustrates the drift in the Mount John system zero point during a night where the zero-point variations were rather extreme. The figure plots the shift (as determined by cross correlation) between Th-Ar spectra obtained throughout the night and a single Th-Ar spectrum taken on the same night. The extent to which this drifting zero point causes an instrumental radial-velocity error $\epsilon_{\rm instr}$ depends on the ability of the mean dispersion solution, obtained from the

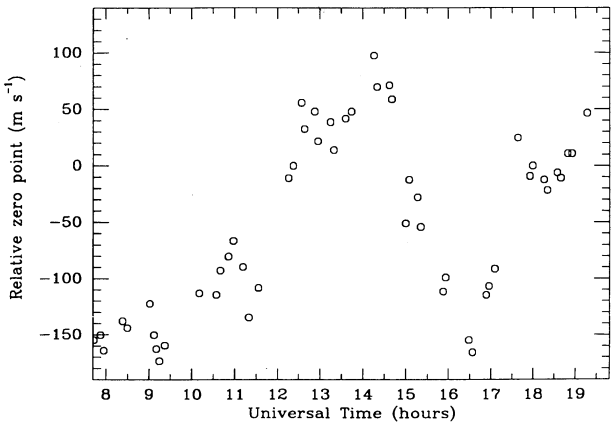

FIG. 1.—Drifts in the zero point of the Mount John system during a night (1991 July 3).

Th-Ar reference spectra exposed before and after each stellar spectrum, to represent the actual changing dispersion solution throughout the stellar exposure. The magnitude of $\epsilon_{\rm instr}$ is therefore expected to be somewhat dependent on the exposure time, since one might expect a linear interpolation between dispersion solutions to be a good approximation over short exposures, but a poorer one over longer exposures, especially if the sky transparency or extinction was changing during the exposure.

3.1.4.1. Air Pressure and Air Temperature Stability

As pointed out by Innis, Isaak, & Isaak (1990), atmospheric pressure or temperature changes cause a change in the refractive index of the air and thus a corresponding change in the wave speed and hence wavelength of light. This will lead to a shift in the positions of spectral lines on the detector. It turns out that an increase in pressure of 1 mbar ($\approx$0.75 mmHg) mimics a velocity shift of about -80 m s^{-1}. Similarly, at a constant pressure of one atmosphere an increase in temperature from 24° C to 25° C mimics a velocity shift of about $+270$ m s^{-1}. Both the temperature-induced shift and the pressure-induced shift are approximately constant over a short length of spectrum so that the net effect for the Mount John program in both cases is an overall uniform shift of the spectrum on the detector.

3.1.4.2. Spectrograph Temperature Stability

Temperature drifts may also cause expansion or contraction of the components in the echelle spectrograph. The most likely origin of a shift in the zero point of the Mount John system from this effect is a change in the tilt of the echelle grating. One side of the grating is attached to the aluminum body of the spectrograph by an aluminum bracket while the opposite side is supported by a steel micrometer which allows adjustment of the grating's tilt. The thermal expansion coefficients of the two metals are markedly different so that the effect of heating or cooling of the spectrograph is a change in the echelle tilt and a subsequent linear shift of the spectrum on the detector. The effect is a shift of about 2000 m s^{-1} °C^{-1}.

A further effect is that of the thermal expansion and contraction of the echelle grating itself. This will change the groove spacing, therefore also changing the dispersion.

3.1.5. *Error in Barycentric Correction, $\epsilon_{\rm bc}$*

The maximum absolute error in the correction applied to reduce the velocities to the frame of the solar system barycenter was calculated to be 6 m s^{-1} over the duration of the Mount John program. The source of this error is the limited number of terms included in the calculation, the smallest of which accounts for the motion of the Sun about the Sun-Jupiter barycenter. The random error in the barycentric correction is about ± 4 m s^{-1}.

Consideration must also be made, however, of the fact that in the Mount John program the barycentric correction was calculated for the mid-time of the stellar exposure, rather than the flux-weighted mean time of the exposure. The two times may be different by a few minutes for rising or setting stars (due to extinction changes) or if the observing is through patchy cloud. For the most part, the mid-exposure time was expected to be within 5 minutes of the mean exposure time. Over this time scale it is the component in the direction to the star of the Earth's motion due to rotation that changes the fastest. This is given by

$$v_{\rm rot} = 465 \cos\delta \sin H \cos\phi \ \text{m s}^{-1} ,$$

where δ is the star's declination, H is the hour angle, and ϕ is the observer's latitude. At Mount John $\cos\phi \approx 1/\sqrt{2}$, so the rate of change of barycentric correction is

$$\partial v_{\rm rot}/\partial H = 329 \cos\delta \cos H \ \text{m s}^{-2} .$$

Considering the worst case at Mount John of an equatorial star at meridian passage with an error in the flux-weighted mean exposure time of 5 minutes (a change in hour angle of $\delta H = 2\pi/(12 \times 24)$ radians), then the error in the barycentric correction would be

$$\epsilon_{\rm bc} = \frac{\partial v_{\rm rot}}{\partial H}\,\delta H \approx 7 \ \text{m s}^{-1} . \quad (2)$$

This is certainly a worst-case error, especially since about two-thirds of the stars in the Mount John program are circumpolar. Estimating the random error from this source as ± 5 m s^{-1}, the total error in the barycentric correction is still only $\epsilon_{\rm bc} = \sqrt{4^2 + 5^2} = 6$ m s^{-1}.

3.2. *Observed Errors*

3.2.1. *Main Features*

Figure 2 comprises a histogram which shows the distribution of observed root mean square (rms) scatters of the velocities $\sigma_{\rm obs}$ for all the stars (including any variables) in the

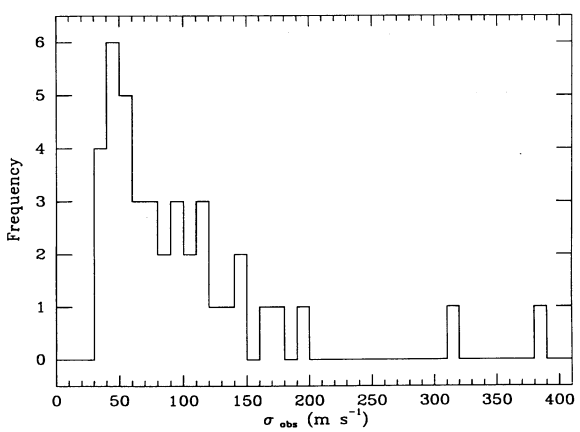

FIG. 2.—Frequency distribution of root-mean-squared scatters $\sigma_{\rm obs}$ of the velocities in the Mount John program.

Mount John program. The main features of the distribution are

1. A peak at about 55 m s^{-1}. Most stars in the program appear in the vicinity of this peak. This clustering of stars toward the left-hand side of the histogram is to be expected if the stars here are intrinsically nonvariable to a few meters per second and the observed velocity scatter is due entirely to the finite precision of the system. The characteristic radial-velocity random error for the system might be described therefore as being about 55 m s^{-1}.

2. A distinct lower bound at about 40 m s^{-1}, which represents the best performance (smallest radial-velocity random error) of the system.

3. An irregular trailing off toward the right-hand side of the histogram (larger rms scatters). The stars here stars are either intrinsically variable or are less precisely observed for some reason.

3.2.2. *Actual Sources of Error*

In no case is the observed rms radial-velocity scatter σ_{obs} of a star in the Mount John program significantly below 40 m s^{-1} over the 2.5 years of the observing program. ϵ_p, ϵ_{disp}, and ϵ_{bc} are therefore eliminated as major contributors to the overall radial-velocity error, since their total contribution to ϵ_v is only about $\sqrt{10^2 + 8^2 + 6^2} = 14$ m s^{-1}. Thus $\epsilon_v^2 \approx \epsilon_{run}^2 + \epsilon_{instr}^2$. The relative contributions of ϵ_{run} and ϵ_{instr} can be assessed noting that the former is expected to be independent of exposure time while the latter is expected to be dependent on it.

In order to see if there is some exposure-time dependence of the precision of the determination of a radial velocity, Figure 3 shows σ_{obs} plotted against stellar magnitude. Since spectra of all stars were recorded with about the same signal-to-noise ratio, any dependence on exposure time should be apparent in this figure. Although Figure 3 is no doubt confused by the presence of stars with variable radial velocity, again the distinct lower bound in rms scatter, presumably due to intrinsically nonvariable stars, is obvious—this time as a clustering along the lower part of the figure. It is apparent, however, that this boundary, which can be interpreted as the radial-velocity error for the system, curves upward toward a greater radial-velocity error for the fainter stars ($V > 4$). This suggests that there is some exposure-time dependence of the radial-velocity precision and therefore that ϵ_{instr} is a major contributor to the overall error in radial-velocity. On the other hand, the brightest stars (α Cen A, α Cen B, α CMi, and γ Cru) were usually observed with exposures of 10 minutes or less. ϵ_{instr} for these stars is expected to be negligible. It is concluded that ϵ_{run} is the dominant source of error for brighter stars.

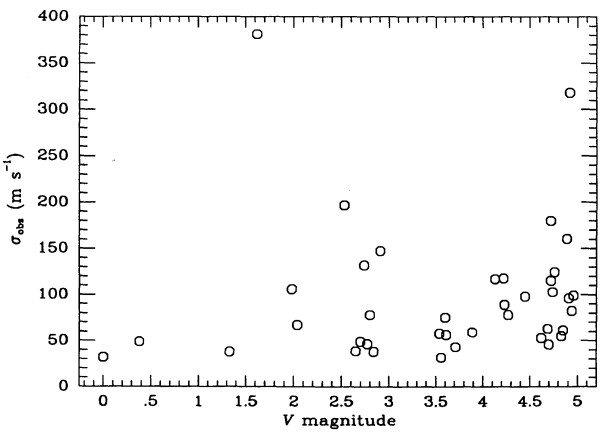

FIG. 3.—Root mean square scatters σ_{obs} of the stars over the duration of the Mount John program plotted against V-magnitude.

In order to verify that run corrections are the major source of the radial-velocity error for bright stars, the rms scatter of velocities of α Cen A, α Cen B, and γ Cru obtained within a single run were calculated. These velocities should be immune to random run correction errors and are displayed in Table 2. During no run was α CMi observed many times so it is not included here, and as γ Cru was found to be variable (Murdoch, Clark, & Hearnshaw 1992), the night analysed for that star was chosen as one where the apparent rate of change of velocity was small.

From just these four examples, it seems likely that the radial-velocity error for the system for bright stars and short time scales is a mere 15 m s^{-1}. This is of the order expected if the only sources of error are ϵ_p, ϵ_{disp}, and ϵ_{bc}. The only explanation for the increase in radial-velocity error for bright stars to about 35–40 m s^{-1} over longer time scales is that run corrections must be applied. Although these were estimated to have a precision of about 17 m s^{-1}, they must be actually closer to 26 m s^{-1} to account for the observed scatter in velocity.

4. TESTS FOR RADIAL-VELOCITY VARIABILITY

Having characterized the sources of radial-velocity errors in the Mount John program, the problem is now to detect any real variations in the radial velocities of the Mount John program stars.

4.1. *F-Test*

The F-test determines whether or not the variances of two distributions are significantly different. F_0 is the ratio of the estimates of the two variances such that $F_0 > 1$ and is associated with a probability $P(F > F_0)$ that one would observe F to be of magnitude F_0 or larger given the number of samples in each distribution and based on the null hypothesis that the variances are equal but F_0 was the observed value by chance.

In the context of determining whether or not a star in the Mount John program is variable in radial velocity, it is required to be known whether the observed variance σ_{obs}^2 of the velocities of each star is significantly different from the variance ϵ_v^2 defined by the presumed random error in radial velocity. F_0 is defined in this case as

$$F_0 = \frac{\sigma_{obs}^2}{\epsilon_v^2} \quad \text{if } \sigma_{obs} > \epsilon_v$$

or

$$F_0 = \frac{\epsilon_v^2}{\sigma_{obs}^2} \quad \text{if } \sigma_{obs} < \epsilon_v .$$

If $\sigma_{obs} > \epsilon_v$, then a small value of $P(F > F_0)$, say $P(F > F_0) < 0.01$, implies that the variance of the observations σ_{obs} is too large to have arisen from an underlying distribution of variance ϵ_v^2, and the star is a candidate radial-velocity variable.

In the Mount John system the value of ϵ_v for each star is not known a priori but it is known (see the previous section) that it arises principally from a constant error from the run corrections ϵ_{run} and an instrumental error dependent on exposure time ϵ_{instr}. It is assumed here that ϵ_{instr} is proportional to the

TABLE 2

FALSE ALARM PROBABILITIES

Star	F-Test $P(F > F_0)$	Frequency[a]	Periodogram $P_1(>z)$	Periodogram $P_2(>z)$	Slope/Curvature $P(>S)$	Slope/Curvature $P(>C)$
HR 77	5.219×10^{-2}	1	2.1×10^{-1}	7.4×10^{-1}	0.740	0.725
HR 98	1.780×10^{-5}	2	1.9×10^{-5}	2×10^{-2}	0.759	0.125
HR 188	2.829×10^{-3}	2	7.6×10^{-4}	5×10^{-2}	0.302	0.171
HR 370	5.231×10^{-1}	2	8.3×10^{-1}	8.7×10^{-1}	0.029	0.215
HR 911	infinitesimal	2	3.3×10^{-50}	0.00	0.473	0.738
HR 1008	4.514×10^{-1}	1	5.9×10^{-1}	7.3×10^{-1}	0.025	0.419
HR 1083	3.623×10^{-11}	1	2.7×10^{-7}	6.3×10^{-1}	0.944	0.677
HR 1136	7.962×10^{-1}	2	8.5×10^{-1}	0.00	0.904	0.342
HR 1674	2.008×10^{-2}	1	5.4×10^{-3}	1.7×10^{-1}	0.193	0.344
HR 1743	7.214×10^{-2}	1	1.0	1.0×10^{-1}	0.670	0.843
HR 1829	6.363×10^{-2}	2	1.0	4.4×10^{-1}	0.864	0.551
HR 1983	1.154×10^{-1}	1	1.3×10^{-2}	3.4×10^{-1}	0.492	0.548
HR 2906	6.471×10^{-2}	1	2.7×10^{-2}	1.0×10^{-1}	0.525	0.350
HR 2943	1.539×10^{-1}	1	1.9×10^{-2}	7.3×10^{-1}	0.996	0.023
HR 3220	2.753×10^{-4}	2	4.1×10^{-2}	9.5×10^{-1}	0.970	0.981
HR 3748	4.620×10^{-31}	2	3.1×10^{-26}	0.00	0.005	0.001
HR 3862	7.735×10^{-1}	1	7.6×10^{-1}	3.0×10^{-2}	0.683	0.511
HR 4134	3.459×10^{-7}	1	2.9×10^{-4}	2.7×10^{-1}	0.351	0.592
HR 4523	4.780×10^{-1}	1	2.1×10^{-1}	0.00	0.639	0.653
HR 4540	9.580×10^{-1}	2	9.9×10^{-1}	5.8×10^{-1}	0.973	0.727
HR 4763	infinitesimal	2	infinitesimal	0.00	0.385	0.159
HR 4786	1.844×10^{-1}	2	3.6×10^{-1}	4.7×10^{-1}	0.975	0.327
HR 4979	7.361×10^{-2}	1	1.0	3.0×10^{-2}	0.759	0.595
HR 5019	1.061×10^{-1}	1	3.4×10^{-2}	9.9×10^{-1}	0.377	0.329
HR 5459	5.066×10^{-2}	2	3.7×10^{-2}	0.00	0.995	0.477
HR 5460	4.896×10^{-2}	2	7.2×10^{-2}	0.00	1.000	0.137
HR 5777	5.428×10^{-2}	2	1.0	2.3×10^{-1}	0.254	0.691
HR 6056	3.330×10^{-38}	2	2.6×10^{-25}	4×10^{-2}	0.000	0.291
HR 6102	8.103×10^{-1}	2	6.2×10^{-1}	5×10^{-2}	0.529	0.455
HR 6603	9.461×10^{-1}	2	9.9×10^{-1}	1.7×10^{-1}	0.017	0.469
HR 6859	7.405×10^{-1}	2	6.0×10^{-1}	1.8×10^{-1}	0.001	0.392
HR 7597	1.262×10^{-2}	1	1.0	$6. \times 10^{-2}$	0.997	0.977
HR 7602	1.222×10^{-1}	2	1.0	5.5×10^{-1}	0.836	0.507
HR 7665	1.781×10^{-3}	2	1.0	1.2×10^{-1}	0.803	0.065
HR 8181	1.512×10^{-5}	1	1.3×10^{-5}	3.8×10^{-1}	0.867	0.105
HR 8232	2.042×10^{-37}	2	1.4×10^{-38}	0.00	0.028	0.000
HR 8387	2.775×10^{-1}	1	1.0	3.6×10^{-1}	0.133	0.888
HR 8447	1.695×10^{-25}	1	6.7×10^{-16}	$9. \times 10^{-2}$	0.836	0.284
HR 8969	2.205×10^{-3}	1	4.0×10^{-2}	9.9×10^{-1}	0.091	0.079

[a] "1" denotes maximum frequency considered $f_{max} = 0.04$ day^{-1}, $M = 80$; "2" denotes $f_{max} = 0.10$ day^{-1}, $M = 200$.

square root of the exposure time and so may be expressed as

$$\epsilon_{instr} \propto \sqrt{t} = \alpha\sqrt{10^{m/2.5}}, \quad (3)$$

where t is the exposure time, α is some constant, and m is the magnitude of the star in the bandwidth of observation (the V-magnitude is close enough for the Mount John system), since $10^{m/2.5}$ is proportional to the exposure time. The functional form of ϵ_v is then known and it may be written as $\epsilon_v^2 = \epsilon_{run}^2 + \alpha^2 10^{m/2.5}$. ϵ_v will therefore be known if ϵ_{run} and α can be determined. Since for nonvariable stars, on average $\sigma_{obs} = \epsilon_v$, ϵ_{run} and α could be found empirically by fitting the relationship

$$\sigma_{obs}^2 = \epsilon_{run}^2 + \alpha^2 10^{m/2.5} \quad (4)$$

to the points corresponding to nonvariable stars in Figure 3. Although the points forming a lower bound in Figure 3 probably correspond to nonvariable stars, it is unclear exactly which points should be included in the fit and which should not be. Indeed there is danger in selecting the points, since if variables are included then the fitted ϵ_v will be too large and the F-test will interpret the σ_{obs} of many stars as being improbably low. On the other hand if some of the nonvariable stars with higher values of σ_{obs} are excluded then the value of the fitted ϵ_v will be too low and the F-test will interpret the σ_{obs} of too many stars as being improbably high (that is, the F-test will predict too many variables). A situation between these two extremes is required and this will be the case where the smallest number of stars have low F-test probabilities. The following procedure was executed

1. Fit equation (4) to (σ_{obs}, m) data base for all the stars in order to determine ϵ_{run} and α and hence ϵ_v.
2. Apply F-test and isolate star with lowest $P(F > F_0)$ because of large σ_{obs}.
3. Discard the star identified in Item 2 from the (σ_{obs}, m) data base and repeat from Item 1.

The best-fit ϵ_v was deemed to be the case where there was the minimum number of stars with $P(F > F_0) < 0.01$.

The final fitted ϵ_v was calculated to be $\epsilon_v = \sqrt{38^2 + 8^2 \times 10^{m/2.5}}$ m s^{-1}. This relationship is plotted in Figure 4. The implied values of $P(F > F_0)$ for each star are listed in Table 3. Fourteen stars had $P(F > F_0) < 0.01$. Since

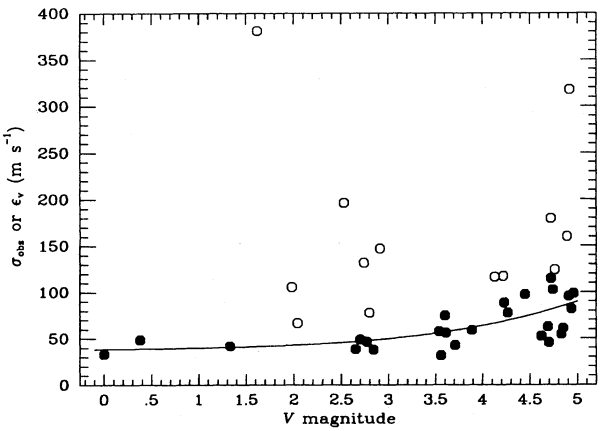

FIG. 4.—Fitted radial-velocity error ϵ_v as a function of stellar V-magnitude (*solid line*). The solid dots are the σ_{obs}-values of stars used in the fit. The open dots are σ_{obs}-values of stars not used in the fit.

there is no physical explanation for a star with an improbably low velocity scatter ($\sigma_{obs} < \epsilon_v$ and $P(F > F_0) < 0.01$), it was expected that all of the stars with $P(F > F_0) < 0.01$ would have improbably high values of σ_{obs}. In fact, one star (HR 7665) did have an improbably small value of σ_{obs}, but since it was only marginal [$P(F > F_0) = 0.0018$], this single anomaly was ignored. The remaining 13 stars were identified by this process as candidate radial-velocity variables, although marginally so in the cases of HR 188 and HR 8969. It is interesting to note that the most convincing variables identified by the F-test are giant or supergiant radial-velocity "standard" stars HR 911, HR 3748, HR 4763, HR 6056, and HR 8232.

4.2. *Power Spectra*

In order to test for embedded periodicities, one can investigate the data in the frequency domain via a Fourier technique. Periodograms were calculated for all the stars in the Mount John program using the method of Lomb (1976) and Scargle (1982), which is appropriate for the analysis of data sampled at unequal intervals. The calculation was made using the computer program of W. A. Lawson (Lawson et al. 1990).

4.2.1. *Lomb-Scargle Probabilities*

In the Lomb-Scargle method, the periodogram is normalized by the variance of the noise in the data such that the height of a periodogram peak can be assigned to a probability that it could have arisen from a spectrum of pure noise. More specifically, if M independent frequencies are scanned in a power spectrum of white noise, the probability that a peak will have a height of z or greater is

$$P(>z) = 1 - (1 - e^{-z})^M . \quad (5)$$

TABLE 3

ROOT MEAN SQUARE SCATTER OF VELOCITIES OF THE BRIGHTEST STARS OBTAINED OVER SMALL TIME SCALES

Star Name	Range in HJD −2440000	Number of Observations	Rms Scatter (m s^{-1})
α Cen A	8130.83–8131.85[a]	9	16
	8323.13–8325.95	6	13
α Cen B	8323.14–8325.96	6	10
γ Cru	8324.89–8325.14	4	15

[a] The six further observations obtained of α Cen A on HJD 2448131 were not included as spectrograph settings were being altered as a test.

A low "false-alarm" probability (say below 0.01) indicates only a small chance that the peak arises by chance from noise.

The Lomb-Scargle false-alarm probabilities for the single highest peaks in the periodograms of the Mount John program stars have been calculated assuming underlying noise values ϵ_v equal to those calculated in § 4.1. That is, the probabilities have been calculated assuming $\epsilon_v = \sqrt{38^2 + 8^2 \times 10^{m/2.5}}$, where m is the V-magnitude of the star. These probabilities are listed in Table 3. For many stars, there were several occasions when the spacing between observations was only a day or so. For these stars, in calculating the false-alarm probability, the power spectrum up to a frequency of 0.10 day^{-1} (period of 10 days) was considered, implying $M \approx 200$ (see discussion of rule-of-thumb calculations of M by Press & Teukolsky 1988). Stars sampled mostly once per run had several observations spaced by about 12 or 13 days, so in calculating false-alarm probabilities for these stars, frequencies only up to 0.04 day^{-1} (period of 25 days) were considered, implying $M \approx 80$.

Since the same underlying noise levels were assumed, it is perhaps not surprising that the Lomb-Scargle false-alarm probabilities below the 0.01 threshold for nearly exactly the same stars that the F-test probabilities were low. The exceptions are that HR 3220 and HR 8969 were marginally nonvariable in the Lomb-Scargle case, and HR 1674 was marginally variable.

4.2.2. *Randomization Test*

The problem with both the Lomb-Scargle probability test and the F-test is that their effectiveness in detecting radial-velocity variability relies on the accuracy in the determination of the underlying radial-velocity error ϵ_v. In order to obtain results that are independent of an assumed ϵ_v, the power spectra obtained above are examined in a slightly different way.

This time, false-alarm probabilities were obtained in a randomization scheme. Retaining the time spacings of the observations of a star, the radial velocities were randomly redistributed amongst the times. One hundred randomized data sets were created for each star and the periodogram of each of these data sets was calculated. The fraction of times the highest peaks in the periodograms of the randomized data sets exceeded the highest peak in the periodogram of the true data set was recorded. This is the false-alarm probability $P_2(>z)$. If the highest peak in the periodogram of the real data is due to a real signal, then the chance that the highest peaks in the 100 randomized data sets are larger is extremely small [small false-alarm probability $P_2(>z)$]. A small false-alarm probability is therefore an indication of a significant peak.

The false-alarm probabilities $P_2(>z)$ for the stars in the Mount John program are listed in Table 3. The stars which appeared as the most striking variables in the previous tests—HR 911, HR 3748, HR 4763, and HR 8232—are also detected as variables in this test although none of the other stars previously detected to be variable are marked as being significant. On the other hand, HR 5459, HR 5460, and HR 4523 are deemed to be significant variables.

The random error in radial-velocity occurs chiefly on two time scales (§ 3.2.2)—a random error from observation to observation and a pseudo-random error from run to run (a systematic error for a given run). This means that those stars for which there were several observations within a run (Case "2" in Table 3) might be flagged as "variable" due to the time scale of the variations between runs. In fact, the low probabil-

ities of three of the case "2" stars—HR 5459, HR 5460, and HR 1136—are due to peaks at around 40–60 days, about the typical time interval between runs. The low probabilities for these stars are therefore discounted as indicators of variability. Furthermore, a similar analysis of the periodogram of HR 4523, having removed the data point with the most positive relative velocity, shows that the periodicity formerly deemed significant all but disappears. Since one point is not a good foundation for a claim of variability, the star is not considered to be variable within the bounds of this test.

4.3. *Slope and Curvature*

Neither the F-test method nor the periodogram method is particularly sensitive to long-term trends in the data. To improve overall detectability, the slope and curvature in each time-series of radial velocities can be analyzed (e.g., Campbell et al. 1988). If S and C are defined respectively as the slope ($\dot{v}$) and curvature ($\ddot{v}$) of the radial-velocity data for a star, determined from independent fits and measured with respective uncertainties ϵ_S and ϵ_C, then the ratios $|S|/\epsilon_S$ and $|C|/\epsilon_C$ are measures of the significance of S and C. These ratios are associated with probabilities $P(>S)$ and $P(>C)$ that the ratios would occur were the data just pure noise. A low value of $P(>S)$ or $P(>C)$ will indicate a candidate variable.

$|S|/\epsilon_S$ and $|C|/\epsilon_C$ were determined for each of the Mount John program stars by the independent fitting of a straight line and a parabola to each time series of radial velocities. The values of ϵ_S and ϵ_C were determined from the scatter of the velocities about the fitted line or curve.

The probabilities $P(>S)$ and $P(>C)$ were determined in a randomization scheme. Retaining the time spacing of the observations of a given star, the radial velocities were randomly redistributed amongst the times. 1500 thus randomized data sets were created for each star. $|S|/\epsilon_S$ and $|C|/\epsilon_C$ were calculated for each of these sets. The probability $P(>S)$ was determined as the fraction of randomized data sets for which $|S|/\epsilon_S$ exceeded the $|S|/\epsilon_S$ of the original data. Similarly $P(>C)$ was defined as the fraction of randomized data sets for which $|C|/\epsilon_C$ exceeded the $|C|/\epsilon_C$ of the original data. This approach has the advantage that no assumptions are made on the distribution of velocity errors.

The resulting values of $P(>S)$ and $P(>C)$ for each star are listed in Table 3, where variables were taken to be those stars for which $P(>S)$ or $P(>C)$ is less than 0.01. Again, HR 3748, HR 6056, and HR 8232 were found to be variable, but in addition HR 6859 was found to have a significant slope.

4.4. *Sensitivity*

In order to assess the sensitivity of the F-test, periodogram and slope/curvature methods to the detection of low-mass companions to the stars in the survey, a series of simulations was performed. Considering the case of a 1 $M_\odot$ primary star, an average orbital inclination ($\langle \sin i \rangle = \pi/4$—see Gray 1976), and circular orbits, radial-velocity curves were generated for a range of periods and companion masses, including an additive Gaussian noise term of 65 m s^{-1} (the mean external radial-velocity error for stars in this program). Each orbit was assigned a random phase and was sampled at 25 epochs which corresponded to the times of the observing runs in the Mount John radial-velocity program. For each grid point corresponding to a single period P and companion mass M_2, 100 orbits were calculated, the difference between them being due to the random phases and the random noise.

For each orbit the false-alarm probabilities for each method were calculated. If, for a particular grid point, the probability was greater than 0.01 for more than 95% of the trials for any given method, that particular (P, M_2) was considered "detectable" by this method. In this manner, the area on the $P-M_2$ plane detectable by any one of the above tests was determined and is shown in Figure 5.

4.5. *Summary of Variables*

None of the tests in this section is completely suitable on its own for a definitive analysis for the presence of orbital motion in the radial-velocity data for the Mount John program. The F-test relies on an accurate estimation of the random error ϵ_v in radial velocity, as does the periodogram analysis if the Lomb-Scargle probability is to be relied upon. The randomization procedure adopted to analyze the periodograms of the data is not dependent on an assumed value for ϵ_v but it does select against finding irregular variations (multiple signals will appear as noise) and it also picks out as a signal the slowly varying error in the run corrections. Finally, the slope and curvature analysis is also independent of an assumed error but is only sensitive to the longer periods.

Of the earliest spectral type dwarfs found to be variable by the F-test—HR 1083 (F3), HR 3220 (F5), HR 4134 (F5), HR 8181 (F7), HR 8447 (F6), and HR 8969 (F7)—none appeared to have a significant peak in its periodogram, and this was confirmed by the randomization probability analysis where none of the F dwarfs was found to be variable. Furthermore none showed significant slope or curvature in their velocities with time. It is possible that the anomalously large velocity scatters of these stars are due not to real variability but merely to having underestimated the radial-velocity random error ϵ_v. It turns out that it is exactly these early F dwarfs which had the broadest cross-correlation peaks. In an F-type star, the smaller number of spectral lines and the increased width of those lines (due to rotational broadening) imply a larger photon-noise limited radial-velocity error (Murdoch & Hearnshaw 1991b). However, even for the broadest-lined and earliest-type stars in this program, for the typical signal-to-noise ratios of the spectra in this program, the photon-noise limited random error was small compared to the total random error (around 100 m s^{-1}). It appears that there is an augmentation of the total error over and above the effect already accounted for in

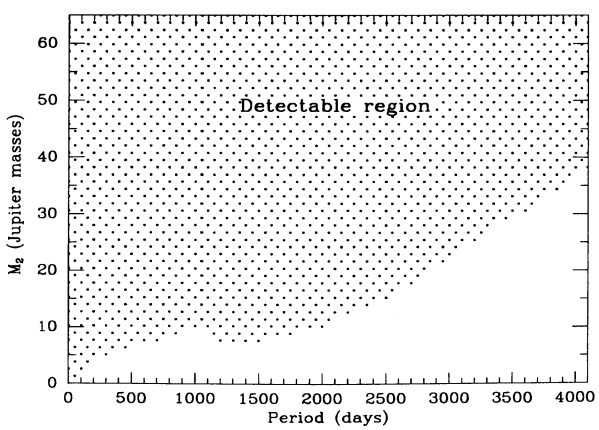

FIG. 5.—Net region of detectability of low-mass companions in the Mount John program, assuming circular orbits, a primary star of 1 $M_\odot$, an average orbital inclination ($\sin i = \pi/4$) and Gaussian noise of 65 m s^{-1}.

the calculation of the photon-noise limited error. This is a phenomenon observed also by Duquennoy, Mayor, & Halbwachs (1991), who find that even though they have calculated the photon-noise limited error and other relevant errors, they need also to add a term dependent on v_{rot} sin i (rotational velocity times sine of the orbital inclination) to obtain a correct total random error. In the case of the Mount John program F dwarfs, the broadening of the spectral lines (as seen in the cross-correlation function peak) is probably also due to rotational broadening, as this is normally a noticeable effect in dwarf spectra to the end of the F class. It is not instructive to compare the estimations of v_{rot} sin i for these stars in the literature, as these are somewhat poor in quality. Another explanation for the broadening could be binarity (the two sets of lines of a double-lined spectroscopic binary may not be resolved, but may appear as a noticeable broadening in the lines of an apparently single spectrum) but one might expect, in this case, a more convincing peak in the periodogram. In summary, the early-type stars indicated above are unlikely to be radial-velocity variables since the relatively large scatter in their radial velocities is probably an artefact of the measurement process rather than true variability.

The most probable variables in the Mount John program are among the giant and supergiant radial-velocity standard stars. HR 3748, HR 6056, and HR 8232 are flagged as variables in every test, while HR 4763 and HR 911 are very convincing variables by both the F-test and periodogram tests, or even by just looking at their velocity records by eye. None of these stars shows a clearly unique signal in its periodogram, although the periodograms of HR 3748 and HR 8232 suggest that a long-period variation is dominant. The complicated periodograms of most of these stars are probably due to irregular intrinsic variability.

The remaining stars found to be variable include HR 98, which was found to be variable by both the F-test and the Lomb-Scargle analysis, although it must be remembered that these two tests are not really independent. The periodogram of HR 98 shows a peak at about 45 days which is not well-defined in height but nevertheless persists despite removal of any small number of points from the periodogram. Because of this and the fact that the velocity sampling is thorough so this is not likely to be an artefact of the window function, HR 98 is considered to be a "possible" variable.

HR 188 was a less convincing variable (it had larger probabilities) in the F-test and Lomb-Scargle analyses and in fact the variability status probably arises from the outlying positions of just 2 points. However, the star is bright, implying small intrinsic velocity scatter, and there is nothing to indicate that there is anything unusual about these two points. HR 188 is thus also given the status of "possible" variable.

Finally, HR 6859 was found to have a significant slope in its velocity time series. This is even apparent from looking at the velocities by eye. Since the number of observations of this star was not large, and the slope of the velocities was small relative to the scatter in the data, its variability is also conservatively designated "possible."

In summary, Table 4 lists the variables and possible variables found in this study. The current findings conflict somewhat with the radial-velocity variability status indicated for many of these stars in The Bright Star Catalogue (Hoffleit 1982). The radial-velocity variability claimed for HR 6056 is confirmed but there is no evidence in this work for the variability claimed for HR 4540, HR 6603, or HR 7602. Furthermore HR 6102 does not appear to be a spectroscopic binary and this study finds no evidence to support the suspected variability of HR 1743, HR 3862, HR 4979, or HR 5460.

TABLE 4

SUMMARY OF RADIAL-VELOCITY VARIABLES

HR Number	Name	Spectral Type
Probable Variables		
HR 911	α Cet	M1.5 IIIa
HR 3748	α Hya	K3 II/III
HR 4763	γ Cru	M3.5 III
HR 6056	δ Oph	M0.5 III
HR 8232	β Aqr	G0 Ib
Possible Variables		
HR 98	β Hyi	G1 IV
HR 188	β Cet	G9 III
HR 6859	δ Sgr	K2.5 IIIa

Campbell et al. (1988) observed possible small long-period changes in the radial velocities of HR 4540, HR 5019, and HR 760. The maximum observed range in radial velocity that they observed for these stars was about 20–30 m s^{-1} over the 6 years of observation at a precision of 13 m s^{-1}. If such variations are real, then they are too small to be confirmed by this study, whose results do not therefore conflict with the Campbell et al. (1988) findings.

5. DISCUSSION

5.1. *The Variable IAU Standard Stars*

The standard stars in the Mount John program found to be variable are α Cet (HR 911; M1.5 III), α Hya (HR 3748; K3 III), γ Cru (HR 4763; M3.5 III), δ Oph (HR 6056; M0.5 III), and β Aqr (HR 8232; G0 Ib). All of these stars were included in the original list of International Astronomical Union radial-velocity standard stars (Pearce 1957) and appear on the revised radial-velocity standard star list of Mayor & Maurice (1985). All are included on the IAU list of future primary standard star candidates (McNally 1988), except for γ Cru which is excluded because of its southerly declination ($-57°$) since the list is restricted to stars within 20° of the celestial equator.

The Mount John program observations suggest that none of these stars should be used as precise radial-velocity standards. Even classical representations of the regions of variability on the Hertzsprung-Russell diagram indicate that the three M giant standard stars are possible small-amplitude red variables. More recent work suggests that the blue edge of the red-variable region extends into the K spectral type, narrowing the gap between the red-variable region and the Cepheid instability strip (Hoffmeister, Richter, & Wenzel 1985; Percy, Landis, & Milton 1989; Walker et al. 1989). Thus even earlier spectral type evolved stars such as α Hya could be intrinsic variables.

5.1.1. *γ Cru, α Cet, and δ Oph*

The Mount John observations of γ Cru are discussed elsewhere (Murdoch et al. 1992). In brief, radial velocities were obtained which spanned about 1500 m s^{-1}. These variations seemed irregular in nature and no clear peak appeared in the periodogram of the velocities but intensive observation within individual runs showed that at least one variation occurred over a time scale that was less than 20 days.

The radial-velocity variations of the other two M-giants in

the Mount John program—α Cet and δ Oph—are of a similar nature to those of γ Cru although these stars were much less intensively observed. Both show highly significant radial-velocity variations, but no unique period in their periodograms. They were both already suspected to be variable in radial velocity—Hoffleit (1982) (δ Oph), Scarfe, Batten, & Fletcher (1989) (α Cet) and in light—Hoffleit (1982) (δ Oph), Eggen (1973) (α Cet). They are probably semi-regular red variables like γ Cru.

5.1.2. α Hya

The Mount John radial-velocity data for α Hya showed that there is a 300 m s^{-1} range in the velocities, which is consistent with the variability reported by Walker et al. (1989). They also found that the star exhibits radial-velocity variability with a total amplitude of about 300 m s^{-1} over their observation period of 5 years and postulated it as a member of a new class of "yellow" intrinsic variables.

5.1.3. β Aqr

The radial-velocity data for β Aqr when plotted (Fig. 6) show the broad minimum of a radial-velocity curve whose period is at least 1000 days or so. Although the data were observed in "clumps" around 4 main epochs, within each clump, data were obtained from between two and seven observing runs. The curvature is therefore not an artefact of systematic differences between runs. It is furthermore not an artefact of the run corrections—the mean of the velocities at each of the four "clumps" has a range of about 300 m s^{-1} and no run correction was as large as this.

β Aqr has too early a spectral type to be a red variable—in fact it lies on or near the Cepheid instability strip, although it is not a Cepheid. The star shows no detectable photometric variability above 0.02 mag (Fernie 1976). The period of the radial-velocity variations program is too long to be due to star spots: such variations would be expected to occur on a time scale close to the rotation period, which has been determined to be 390 days by Brosius, Mullan, & Stencel (1985) from variations in Ca II H and K emission. The period of the variations also seems to be too long to be related to Cepheid pulsation, although assuming a sinusoidal radial-velocity curve with period 1000 days and semi-amplitude 150 m s^{-1}, the implied radius change (around 8% of the about 75 $M_\odot$ stellar radius) is not unreasonable for a radial pulsator. If the variations are real, it seems most likely that they are due to orbital motion with a companion, rather than to intrinsic variability of the star.

β Aqr has an 11th magnitude optical companion at a separation of 35".5 (Hoffleit 1982). Since the spectroscopic parallax of β Aqr implies that it is 300 pc distant (Hirshfeld & Sinnott 1982, p. 548), if the association of the visual pair is physical, then the companion is probably something like an F5 dwarf (mass about 1.4 $M_\odot$) and the period of their common orbit a matter of tens of thousands of years. The chance that the minimum of the radial-velocity curve of this orbit was observed over the course of the Mount John program is small enough that the visual companion can be eliminated as a possible cause of the radial-velocity variations.

As less than one cycle was observed in the data, a reliable estimate of the period and semi-amplitude of the orbit cannot be made in order to derive a companion mass. The lower limit to the period is around 1000 days, which does at least imply an orbit well outside the approximately 75 $R_\odot$ star, assuming that the mass of the star is about 8 $M_\odot$ (Parsons & Bouw 1971). The minimum semi-amplitude of the orbit is about 150 m s^{-1}.

In order to consider what companion mass the data might imply, circular orbits of various periods were fitted to the data. Figure 7 shows how the period of the orbit is related to the value of $M_2 \sin i$. Without knowledge of the orbital inclination, one can only say that there is a possibility of the companion being substellar (less than 0.08 $M_\odot$) as long as the period is less than about 2200 days.

There is some knowledge of the inclination of β Aqr's rotational axis and if one is prepared to make the assumption that the orbital and rotational axes are parallel (Campbell & Garrison 1985), then this can put a further constraint on the likely mass of the companion. Gray & Toner (1987) have calculated $v \sin i$ to be 6.3 ± 1.3 km s^{-1} from an analysis of line profiles. Using this value, the rotation period of 390 days, and a stellar radius of 75 $R_\odot$, the implication is that the rotational axis has an inclination of $\sin i = 0.65$. Assuming that this value can be adopted for the orbital inclination, the period of the circular orbit can be a maximum of 1800 days before the implied companion mass is stellar.

5.2. Limits to Companion Masses in the Mount John Program

The radial-velocity perturbation induced by a brown-dwarf companion to a solar-mass star with a period less than 10 years is between a few hundred and a few thousand meters per

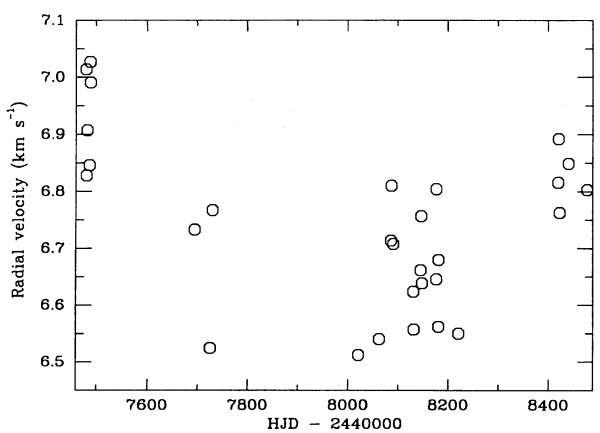

FIG. 6.—Mount John program time series of radial velocities for β Aqr

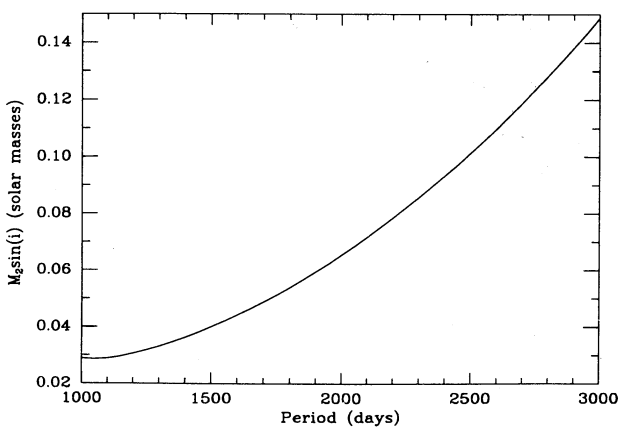

FIG. 7.—Dependence of mass of implied companion to β Aqr on best-fit circular orbits of different periods, assuming a primary mass of 8 $M_\odot$.

second for all inclinations except those nearly in the plane of the sky. Since the characteristic radial-velocity error in the Mount John program is about 55 m s^{-1}, any perturbation with a period of a few years and amplitude of the order of a couple of hundred meters per second or more should be easily discernible in the radial velocities of the primary star. In other words, if brown dwarfs are common as companions to solar-type stars then radial-velocity perturbations should have been obvious in the time series of velocities of some of the Mount John program stars. In fact, the only obvious previously undiscovered single-lined spectroscopic binary was HR 3220, whose companion is stellar. The lack of any other obvious spectroscopic binary is alone a strong negative statement regarding the presence of brown-dwarf companions to the Mount John program stars.

In § 4 the status of radial-velocity variability of the Mount John program stars was examined by using tests which were aimed at the detection of very low amplitude variations in radial velocity. Only a single dwarf star (β Hyi) was indicated to be variable and even so its variability status is somewhat marginal. Note that the Figure 5 summary of the detectable orbits for the Mount John program used a slightly pessimistic radial-velocity error of 65 m s^{-1}. Furthermore the calculation is for average orbital inclination and so for a given companion mass, the program could detect longer period orbits for more favorably inclined systems (i closer to 90°). Finally, the shaded area represents detectability at the 95% confidence level. In practice, the probability of detecting an orbit decreases smoothly over the boundary from the shaded region, meaning that orbits are in fact detectable in the unshaded region, but with a smaller probability.

The program should have found all companions with masses greater than 10 $M_{2\downarrow}$ and periods shorter than 2000 days (5.5 years). If the lower mass boundary for brown dwarfs is about 20 $M_{2\downarrow}$, it can be said that all companions of brown-dwarf mass or greater with periods shorter than 3000 days (8.2 yr) should have been found. In other words, apart from the possibility of a companion to β Hyi, it is very unlikely that brown dwarfs with periods less than 8 years are in orbit about the dwarf stars in the Mount John program. On the other hand, two of the evolved IAU standard stars (β Aqr, a G0 supergiant, and δ Sgr, a K giant) showed long-period radial-velocity modulation that could be due to low mass companions. The only effects that could conceivably mask significant numbers of companion brown dwarfs from detection are preferential orientation of their orbits in the plane of the sky or that they have large eccentricities (in very eccentric orbits the stellar velocities change only very slowly—perhaps imperceptibly—over most of the orbit and one might not be observing when the rapid changes in velocity occur at periastron passage) and a longitude of periastron close to $\pm 90°$. However, these effects can be discounted as they assume the Sun is in a favored position.

A stronger statement concerning the existence of companion brown dwarfs can in principle be made by considering astrometric data. While radial-velocity analyses such as the Mount John program are more sensitive to shorter period orbits, astrometric analyses are more sensitive to longer period ones. A star which has been included in a long-term astrometric program will have a determinable upper limit to possible perturbations due to a companion, over periods comparable to the length of the astrometric survey. Since the companion mass is proportional to the astrometric perturbation, knowledge of the maximum likely astrometric perturbation gives an estimate of the maximum likely companion mass. At long periods, this maximum companion-mass limit is inevitably a stronger constraint on the nature of possible companions than is the maximum companion-mass limit set by radial velocities.

Unfortunately the long-term astrometric coverage of southern hemisphere stars is very poor and the authors are aware of only four stars in this sample for which an astrometric limit to perturbations exists. These are α Cen A, α Cen B, and α CMi (Procyon) (due to the measurements of their visual orbits) and δ Eri (which is included in the study of long-term astrometric perturbations by Lippincott & Worth 1980). No astrometric perturbation other than the visual orbit has been observed in either the α Cen system from over 100 years of data or the Procyon system from 34 years of data (Strand 1951). Again, no astrometric perturbation has been found in the orbit of δ Eri by Lippincott & Worth (1980) from 38 years of data. These results are interpreted to mean in each case a maximum angular perturbation due to an unseen companion (a third companion in the case of the α Cen and Procyon systems) of 0.″02. The value of 0.″02 is chosen (following the reasoning of Marcy & Benitz 1989) because a perturbation would have to be several times larger than the typical error in the program to be discovered. The value of 0.″02 is about 3 times the typical positional error in the relevant photographic astrometry programs in this case.

From this information, astrometric limits to the masses of possible companions were determined for α Cen A and B, Procyon, and δ Eri. Assuming circular orbits, the minimum detectable mass via astrometry is $M_2 = (M_1/P)^{2/3}\theta/\pi_p$, where M_1 and M_2 are the primary and secondary masses respectively, P is the period of the orbit, θ is the maximum likely astrometric perturbation for the system, and π_p is the system parallax. Table 5 shows the data used for this calculation. Figure 8 shows the upper limits to the masses of companions of the four stars derived from astrometry, along with the area in the $P-M_2$ plane where companions are eliminated in this radial-velocity program (from Figure 5). Even though the maximum angular perturbation for each star was assumed to be the same, the placement of the upper limit line differs for each star mainly because of the stars' different distances.

It can be seen that for both α Cen A and α Cen B, no companion of mass greater than about 10 $M_{2\downarrow}$ exists with a period up to the duration of the astrometric coverage of the system which is more than a century. α CMi has no companion of mass greater than about 24 $M_{2\downarrow}$ and period shorter than 34 years and δ Eri has no companion of mass greater than about 32 $M_{2\downarrow}$ and period less than 38 years. Despite the fact that δ Eri has the highest upper mass limit, it is this star for which this calculation has most significance, since long-period orbits would not be expected about α Cen A, α Cen B, and α CMi

TABLE 5

DATA USED TO DERIVE COMPANION MASS LIMITS

Star	π_p[a]	Reference	M_1[b]	Reference
α Cen A	+0.750	Hoffleit 1982	1.09	Heintz 1982
α Cen B	+0.750	Hoffleit 1982	0.90	Heintz 1982
α CMi	+0.292	Hoffleit 1982	1.74	Strand 1951
δ Eri	+0.113	Hoffleit 1982	0.79	Lang 1992

[a] All parallaxes are trigonometric.

[b] The mass of δ Eri is based on its spectral type, the other masses are from the visual orbits.

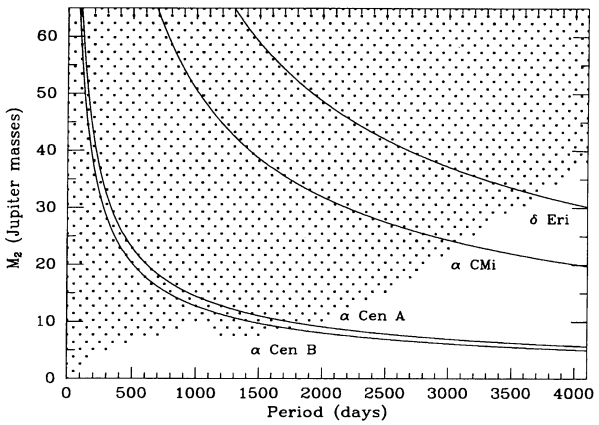

FIG. 8.—Limits to masses of companions of α Cen A, α Cen B, α CMi, and δ Eri. The upper limit to the mass of companions as determined by this program is the boundary of the shaded region, while the lines are the upper mass limits as determined by astrometry.

because of the latter stars already having stellar companions in long-period orbits.

5.3. *Status of the Existence of Brown Dwarfs*

In the Mount John program no certain brown dwarf companion and only one possible brown-dwarf companion (to β Hyi) was found despite sensitivity to brown-dwarf companions of any mass with a period less than 8.2 years (orbital distance less than 4 AU).[2] It can be said that close brown-dwarf companions to the Mount John program stars are therefore at the least, rare. The Mount John program sample is not large, but because the stars are all typical solar-type dwarfs it could be suggested that brown dwarfs closer than 4 AU are rare in orbit around any solar-type dwarf. This conclusion is strengthened by almost identical results from other radial-velocity searches (Campbell et al. 1988; Tokovinin 1988; Marcy & Benitz 1989; Mazeh et al. 1990). Duquennoy & Mayor (1991) have estimated the substellar companion frequency to solar-type stars as $8 \pm 6\%$. Although the dwarf stars in the Mount John program do not form a complete sample like those in the Duquennoy & Mayor (1991) study, from their results, out of the 29 dwarfs in this program one would expect 2.3 ± 1.7 stars with radial-velocity variations suggesting possible brown dwarf companions. The single possible brown dwarf in the Mount John program is therefore consistent with the Duquennoy & Mayor (1991) results.

While dynamical surveys (such as the radial-velocity ones above) have found only a few candidate brown-dwarf companions to stars, the few brown-dwarf companion candidates which have arisen from photometric searches (Skrutskie et al. 1986, 1989; Forrest et al. 1989; Rieke & Rieke 1990) are not clearly distinguishable from low-mass stars. Marcy & Benitz (1989) have pointed out that these results are very significant when viewed together, since radial-velocity, astrometric, and photometric methods are complementary: radial-velocity methods being sensitive to orbits within about 5 AU of the primary, astrometric methods covering 5–10 AU and photometric searches being sensitive from about 10 to nearly 50 AU.

Further interpretation of the results of searches for brown dwarfs as companions to stars is facilitated by noting that brown dwarfs are generally considered to form like stars and as such, might be expected to have the same orbital characteristics that stars have. A recent result on stellar companions to stars is that the frequency distribution of periods of binary systems approximates a broad bell-shaped curve peaking at 180 years and is independent of the companion mass (Duquennoy & Mayor 1991). If the orbital characteristics of stellar companions also apply to brown-dwarf companions then these results imply that if brown dwarfs exist as companions to stars, the most common period of such binary systems would be about 180 years. This corresponds to an orbital separation of about 30 AU for solar-type stars. Since orbital separations of up to about 50 AU have been investigated by brown-dwarf searches to date, companion brown dwarfs have been looked for in the majority of their likely orbital habitats.

The existence of significant numbers of brown-dwarf companions has not been ruled out completely. Brown-dwarf companions to stars which are old or of low mass would not necessarily have been discovered in orbits with separations larger than 10 AU because their low luminosities would cause difficulties for photometric searches. The existence of larger numbers of low-mass brown dwarfs than the apparently rare higher-mass brown dwarfs would suggest either a bimodal mechanism of starlike formation by fragmentation (one mechanism for stellar masses and another for substellar masses) or simply that the upper limit for masses formed like planets is in the brown-dwarf mass range. These hypothetical low-mass brown dwarfs might in the latter case more properly be called planets.

Furthermore, brown dwarfs could still abound in the field. Mazeh et al. (1992) have commented that the secondary mass function for close binaries is quite different from the field star mass function at low masses. The secondary mass function of Mazeh et al. (1992) appears below 1 $M_\odot$ to be flat or decreasing towards lower masses. The implication of a small number of companion brown dwarfs is in agreement with the results of this and other radial-velocity programs. The field star mass function, however, appears in most studies to be increasing towards lower masses, at least as far as 0.3 $M_\odot$ (e.g., Kroupa, Tout, & Gilmore 1990), leaving open the interpretation that the number density of field brown dwarfs might be greater than that of companion brown dwarfs. Again, observations are hampered by the difficulties in photometric detection of low-mass and old brown dwarfs.

It is unclear, given the current results of searches to brown dwarfs, whether brown dwarfs could make up Bahcall's (1984) 100 $M_\odot$ pc^{-3} of "missing mass" in the solar neighborhood, although it appears unlikely that this could be provided by higher mass brown dwarfs in binary systems. Kuijken & Gilmore (1989), however, have suggested that the local missing mass problem might not exist anyway. If this is true, then much of the motivation behind the suspicion of large numbers of (presumably field) brown dwarfs disappears.

Evidence for massive halos, on the other hand, is still overwhelming. The problem has been examined theoretically whether these massive halos could be made up of baryonic matter. The general answer is that they cannot, unless the matter is in compact objects (like brown dwarfs). The possibility of the existence of brown dwarfs in the halo has not yet been ruled out (Adams & Walker 1990). These might be looked for by searches for the gravitational microlensing of Magellanic Cloud stars (for example Gott 1981).

[2] More massive brown dwarfs at greater orbital distances would have been discovered, for example all 45 $M_\odot$ objects out to 5 AU (equivalent to the orbit of Jupiter) or all 80 $M_\odot$ objects out to 6 AU.

K. A. M. acknowledges the support of a New Zealand Vice Chancellor's Committee Scholarship, a Ministry of Research Science and Technology Women's Study Award, a Zonta International Amelia Earhart Award, and a Smithsonian Predoctoral Fellowship.

REFERENCES

Adams, F. C., & Walker, T. P. 1990, ApJ, 359, 57
Bahcall, J. N. 1984, ApJ, 276, 169
Barden, S. C. 1988, in Fiber Optics in Astronomy, ed. S. C. Barden (San Francisco: ASP), 40
Boss, A. P. 1986, in Astrophysics of Brown Dwarfs, ed. M. C. Kafatos, R. S. Harrington, & S. P. Maran (Cambridge: Cambridge Univ. Press), 206
Brosius, J. W., Mullan, D. J., & Stencel, R. E. 1985, ApJ, 288, 310
Campbell, B., & Garrison, R. F. 1985, PASP, 97, 180
Campbell, B., Walker, G. A. H., & Yang, S. 1988, ApJ, 331, 902
Duquennoy, A., & Mayor, M. 1991, A&A, 248, 485
Duquennoy, A., Mayor, M., & Halbwachs, J.-L. 1991, A&AS, 88, 281
Eggen, O. J. 1973, ApJ, 186, 793
Fernie, J. D. 1976, PASP, 88, 116
Forrest, W. J., Garnett, J. D., Ninkov, Z., Skrutskie, M., & Shure, M. 1989, PASP, 101, 877
Forrest, W. J., Skrutskie, M. F., & Shure, M. 1988, ApJ, 330, L119
Gott, J. R. 1981, ApJ, 243, 140
Gray, D. F. 1976, The Observation and Analysis of Stellar Photospheres (New York: Wiley), 405
Gray, D. F., & Toner, C. G. 1987, ApJ, 322, 360
Griffin, R., & Griffin, R. 1973, MNRAS, 162, 243
Heintz, W. D. 1982, Observatory, 102, 42
Henry, T. J., & McCarthy, D. W., Jr. 1990, ApJ, 350, 334
———. 1992, in IAU Colloq. 135, Complementary Approaches to Double and Multiple Star Research, ed. H. A. McAlister & W. I. Hartkopf (San Francisco: ASP), 10
Hirshfeld, A. H., & Sinnott, R. W., eds. 1982, Sky Catalogue 2000.0 (Cambridge: Cambridge Univ. Press)
Hoffleit, D. 1982, The Bright Star Catalogue (New Haven: Yale Univ. Obs.)
Hoffmeister, C., Richter, G., & Wenzel, W. 1985, Variable Stars (Berlin: Springer)
Innis, J. L., Isaak, G. R., & Isaak, K. 1990, Observatory, 110, 188
Irwin, A. W., Fletcher, J. M., Yang, S. L. S., Walker, G. A. H., & Goodenough, C. 1992, PASP, 104, 489
Jameson, R. F., Sherrington, M. R., & Giles, A. B. 1983, MNRAS, 205, 39P
Jameson, R. F., & Skillen, I. 1989, MNRAS, 239, 247
Kuijken, K., & Gilmore, G. 1989, MNRAS, 239, 651
Kumar, C. K. 1987, AJ, 94, 158
Kroupa, P., Tout, C. A., & Gilmore, G. 1990, MNRAS, 244, 76
Lang, K. R. 1992, Astrophysical Data: Planets and Stars (New York: Springer), 132
Lawson, W. A., Cottrell, P. L., Kilmartin, P. M., & Gilmore, A. C. 1990, MNRAS, 247, 91
Lippincott, S. L., & Worth, M. D. 1980, AJ, 85, 171
Lomb, N. R. 1976, Ap&SS, 39, 447
Marcy, G. W., & Benitz, K. J. 1989, ApJ, 344, 441
Mayor, M., & Maurice, E. 1985, in IAU Colloq. 88, Stellar Radial Velocities, ed. A. G. D. Philip & D. W. Latham (Schenectady: L. Davis Press), 299
Mazeh, T., Latham, D. W., Stefanik, R. P., Torres, G., & Wasserman, E. 1990, in NATO Advanced Study Institute on Active Close Binaries, ed. C. İbanoğlu (Dordrecht: Kluwer), 267
Mazeh, T., Goldberg, D., Duquennoy, A., & Mayor, M. 1992, ApJ, 401, 265
McNally, D., ed. 1988, Trans. IAU, 20b, 267
Murdoch, K., Clark, M., & Hearnshaw, J. B. 1992, MNRAS, 254, 27
Murdoch, K., & Hearnshaw, J. B. 1991a, Ap&SS, 186, 169
———. 1991b, Ap&SS, 186, 137
———. 1993, Observatory, in press
Parsons, S. B., & Bouw, G. D. 1971, MNRAS, 152, 133
Pearce, J. A. 1957, Trans. IAU, 9, 441
Percy, J. R., Landis, H. J., & Milton, R. E. 1989, PASP, 101, 893
Press, W. H., & Teukolsky, S. A. 1988, in Computers in Physics, Nov/Dec, (New York: AIP), 77
Rieke, G., & Rieke, M. J. 1990, ApJ, 362, L21
Scarfe, C. D., Batten, A. H., & Fletcher, J. M. 1989, PDO, 18, 21
Scargle, J. D. 1982, ApJ, 263, 835
Skrutskie, M. F., Forrest, W. J., & Shure, M. 1986, in Astrophysics of Brown Dwarfs, ed. M. C. Kafatos, R. S. Harrington, & S. P. Maran (Cambridge: Cambridge Univ. Press), 82
———. 1989, AJ, 98, 1409
Stauffer, J., Hamilton, D., Probst, R., Rieke, G., & Mateo, M. 1989, ApJ, 344, L21
Strand, K. A. 1951, ApJ, 113, 1
Tarter, J. C. 1975, Ph.D. thesis, Univ. California–Berkeley
Tokovinin, A. A. 1988, ApJ, 28, 173
Walker, G. A. H., Yang, S., Campbell, B., & Irwin, A. W. 1989, ApJ, 343, L21
Zuckerman, B., & Becklin, E. E. 1987, ApJ, 319, L99